

DrugClaw and DrugAudit: A Primary-Source-Grounded Agent and Authority-Aware Benchmark for Drug-Information Question Answering

Qing Wang^{1*}, Bo Li^{2*}, Jialu Liang¹, Daling Shi¹, Bob Zhang², Qianqian Song^{1#}

¹Department of Health Outcomes and Biomedical Informatics, College of Medicine, University of Florida, Florida, USA

²PAMI Research Group, Department of Computer and Information Science, Faculty of Science and Technology, University of Macau, Taipa, Macau, China

*Co-first authors. #Correspondence: qsong1@ufl.edu

Abstract

Drug-information question answering is a high-stakes setting where hallucinated facts can mislead clinical decision-making and the provenance of each cited fact matters as much as the fact itself. We present DrugClaw, a multi-agent retrieval-augmented system that queries a registry of drug and pharmacovigilance skills via a reflection-driven state-machine workflow and returns answers grounded in primary regulatory or peer-reviewed records. We also contribute DrugAudit, a 3,772-item authority-aware benchmark with an evaluation panel that scores upstream-of-gold source match, token-level semantic snippet overlap, and citation faithfulness under a dual-judge LLM-as-judge protocol with inter-judge $\kappa = 0.88$ (almost-perfect). Across DrugAudit plus drug-related subsets of MedQA (751) and PubMedQA (512), DrugClaw is top-1 on every column of the headline table: composite Evidence Index under both judges, judge-mediated answer correctness, primary-source rate (0.918, +10.1 pp over next-best), faithfulness (0.887, +5.9 pp), MedQA (0.920), and PubMedQA (0.693).¹

1 Introduction

When a clinician asks whether a drug has a measured EC₅₀ against a target, how a label warns about hepatotoxicity, or what adverse events have been reported to FAERS, an incorrect answer is a patient-safety liability, not merely a benchmark loss. Large language models show strong general biomedical knowledge (Singhal et al., 2023; Nori et al., 2023; Luo et al., 2022; Taylor et al., 2022), but their parametric knowledge degrades quickly outside high-resource diseases (Ren et al., 2025), they offer no native audit trail to a regulatory or peer-reviewed source, and they hallucinate plausible-looking numerics with regularity (Ji et al., 2023; Maynez et al., 2020).

¹<https://anonymous.4open.science/r/DrugClaw-01A3/README.md>

Tool-augmented agents (Huang et al., 2025; Gao et al., 2024; OpenAI, 2025a) partially close this gap, but on drug-information tasks two failure modes are endemic. Tool-rich systems often skip the regulatory primary source and cite whichever URL the search returns first; bare LLMs answer fluently without citations and fabricate plausible numerics. A deeper gap is at the *evaluation* layer: existing biomedical QA scoring grades surface answer correctness but does not distinguish a citation to an FDA Label from a citation to a downstream aggregator wrapper of that same Label – the very distinction that anchors evidence-based medicine reporting standards (Page et al., 2021; Guyatt et al., 2008; Guideline, 2003). In regulated drug-information settings, provenance is not a presentation choice but an evaluation axis.

This paper makes four contributions.

DrugClaw, an authority-grounded multi-agent system. DrugClaw (Figure 1) is a reflection-driven state-machine over eight specialised agents that queries a registry of fifty-seven active drug and pharmacovigilance skills drawn from a fifteen-subcategory tree of over seventy catalogued resources. The system ships in three reasoning modes (linear, graph, web-only) and every emitted answer carries a structured evidence list whose source URLs point back to primary regulatory or peer-reviewed records.

DrugAudit and an authority-aware metric panel. Three structural biases in prior drug-QA scoring motivate it: strict source-name canonicalisation that penalises upstream primary sources (CPIC for a PharmGKB query, FAERS for a SIDER query); substring-only snippet matching that fails when gold snippets are field names rather than sentences; and the absence of a citation-quality signal distinct from citation presence. We address these with an equivalence-bucket rule, a token-Jaccard semantic overlap, and a faithfulness rate (§4).

A dual-judge LLM-as-judge protocol. Llama-3.1-70B-Instruct (primary) and gpt-oss-120b (secondary) are external to every candidate system, eliminating direct self-evaluation bias (Zheng et al., 2023; Panickssery et al., 2024). Across 22,471 parseable paired verdicts (of 26,404 attempted) we obtain macro $\kappa = 0.88$, which corresponds to almost-perfect agreement under Landis and Koch (1977).

Comprehensive empirical comparison. We evaluate seven systems (DrugClaw (linear), DrugClaw (graph), Biomni (Huang et al., 2025), DeepEvidence (Wang et al., 2025), ToolUniverse (Gao et al., 2024), and direct LLMs at two scales) on 3,772 items spanning nine source-database subsets plus drug-related MedQA and PubMedQA. DrugClaw is top-1 on every column of the headline table (Table 1).

2 Related Work

Biomedical question answering and tool agents. Medical QA benchmarks span clinical reasoning (MedQA, Jin et al., 2021; MedMCQA, Pal et al., 2022), literature QA (PubMedQA, Jin et al., 2019; BioASQ, Krithara et al., 2023) and clinical-note tasks (Abacha et al., 2017); Med-PaLM (Singhal et al., 2023) and GPT-4 (Nori et al., 2023) close much of the multiple-choice gap without providing verifiable citations. Tool-augmented agents (Schick et al., 2023; Yao et al., 2023; Patil et al., 2024; Qin et al., 2024) close a different gap, with chemistry (ChemCrow, M. Bran et al., 2024) and biomedical (Biomni, Huang et al., 2025; ToolUniverse, Gao et al., 2024; TxAgent, Gao et al., 2025) instantiations scaling to hundreds of tools. Specifically on drug tasks, DrugAgent (Liu et al., 2024a) casts drug discovery as multi-agent collaboration, MedAdapter (Shi et al., 2024) performs test-time adaptation for medical reasoning, DrugWatch (Bobrov et al., 2024) visualises FAERS-grounded drug-safety retrieval, and deep-research style agents (OpenAI, 2025a) interleave web search with citation synthesis. ChemCrow targets synthesis planning, Almanac (Zakka et al., 2024) retrieves guideline passages, and TxAgent’s tool stack is largely subsumed by ToolUniverse, so we adopt Biomni, DeepEvidence (Wang et al., 2025) and ToolUniverse as the directly comparable agentic baselines. DrugClaw differs in two respects: its primary retrieval channel is a closed registry of vetted regulatory and peer-reviewed sources rather than

an open-web index (with a web-search fallback quantified in Appendix E), and its evidence schema constrains every claim to carry a primary-source URL rather than a loose web reference.

Retrieval-augmented generation in medicine. Retrieval-augmented generation (Lewis et al., 2020) and its self-reflective (Asai et al., 2024) and graph-structured (Wu et al., 2025) variants have been adapted to clinical settings most visibly by Almanac (Zakka et al., 2024) and the medical retrieval-augmented benchmark of Xiong et al. (2024); Ren et al. (2025) characterise the factual-knowledge boundary of LLMs that motivates retrieval over parametric recall. DrugClaw sits at the structured-record end of this spectrum. It queries typed records from regulatory and peer-reviewed databases and treats the database row itself as the citation, rather than retrieving passages from free text. Almanac in particular (Zakka et al., 2024) retrieves over a closed corpus of clinical guidelines with physician-graded answer quality; its citation unit is a guideline passage rather than a primary regulatory record, and its evaluation does not separate upstream-primary from aggregator-wrapper provenance. DrugClaw and Almanac therefore target complementary evidence universes: regulatory and pharmacovigilance records in our case, clinical guidelines in theirs. Our authority-aware panel (§4) operationalises the upstream-vs-aggregator distinction that the guideline-passage unit cannot express.

Citation-faithfulness evaluation. Most retrieval-augmented evaluations score retrieval through recall-at- k (Karpukhin et al., 2020) or generation through BLEU, ROUGE or LLM-as-judge. Citation faithfulness for general-domain generation (Gao et al., 2023; Min et al., 2023; Manakul et al., 2023) focuses on whether claims are supported but not on the *authority* of the cited source, that is, whether the citation points to the upstream FDA record or a downstream aggregator wrapper. Our primary-source rate and upstream-equivalence rule (§4) make this distinction explicit and judge-independent.

LLM-as-judge methodology. Zheng et al. (2023) and Liu et al. (2023) established LLM-as-judge as a scalable substitute for human ratings; follow-up work has documented self-preference and length bias (Liu et al., 2024b; Panickssery et al., 2024). We mitigate these biases by choosing judges (Llama-3.1-70B-Instruct and gpt-oss-120b)

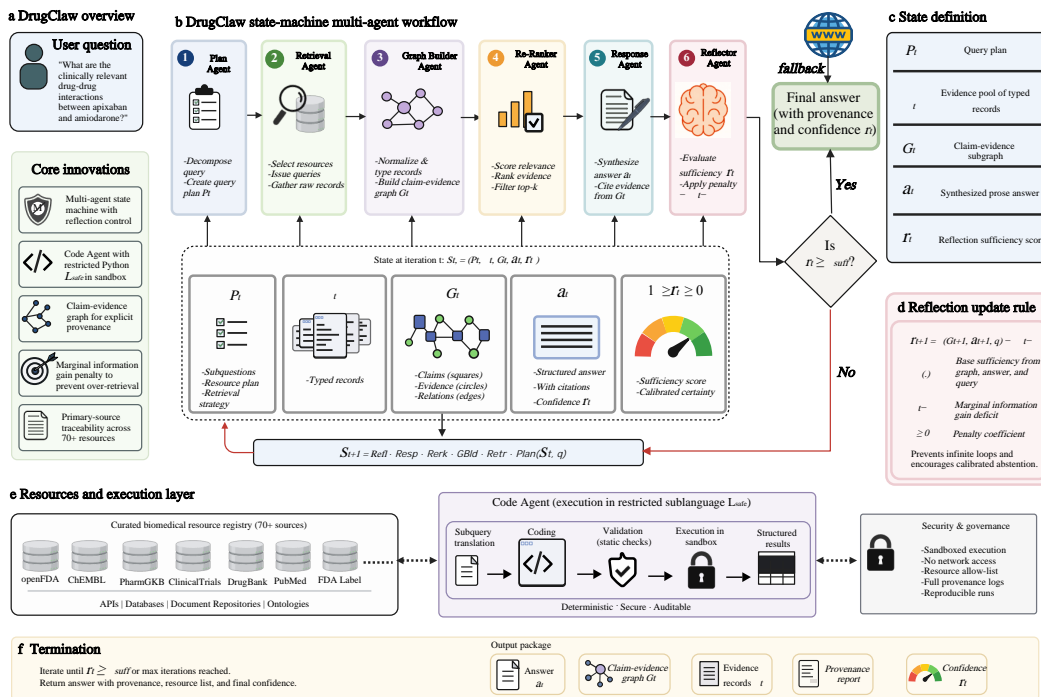


Figure 1: **DrugClaw architecture.** **a**, Motivating clinical query and the core innovations: multi-agent state machine with reflection, sandboxed Code Agent, claim-evidence graph, regression-penalised reflection update, and primary-source traceability across 70+ resources. **b**, State-machine workflow: six agents (Plan, Retrieval, Graph Builder, Re-Ranker, Response, Reflector) iterate $\mathcal{S}_{t+1} = \text{Refl} \circ \text{Resp} \circ \text{Rerk} \circ \text{GBld} \circ \text{Retr} \circ \text{Plan}(\mathcal{S}_t, q)$ until $r_t \geq \tau_{\text{suff}}$, with a web-search fallback invoked on terminal insufficiency. **c**, State components $\mathcal{S}_t = (\mathcal{P}_t, \mathcal{E}_t, \mathcal{G}_t, a_t, r_t)$: query plan, typed evidence pool, claim-evidence subgraph, prose answer, and reflection sufficiency. **d**, Reflection update $r_{t+1} = \rho_{t+1} - \lambda \Delta_t^-$ with $\Delta_t^- = \max(0, r_t - \rho_{t+1})$, where the regression penalty discourages thrashing across iterations (App. B). **e**, A 70+ source registry (openFDA, ChEMBL, PharmGKB, ClinicalTrials.gov, DrugBank, PubMed, FDA Label, ...) is reached only via the Code Agent’s deterministic, sandboxed pipeline (translate \rightarrow code \rightarrow validate \rightarrow execute \rightarrow return structured results). **f**, Termination: iterate until $r_t \geq \tau_{\text{suff}}$ or max iterations; output answer, claim-evidence graph, evidence records, provenance, and confidence r_t .

whose model families do not appear in any candidate system, and by reporting Cohen’s κ across the pair as a calibration check.

3 The DrugClaw System

DrugClaw (Figure 1) is a state-machine workflow. Its eight specialised agents, comprising the six iteration-loop operators of Equation 1 together with a Code Agent and a web-search fallback, operate over a closed registry of drug-information skills. The architecture realises three design goals that prior biomedical agents only partially satisfy: *primary-source traceability*, requiring every emitted claim to carry an identifier resolvable against a primary regulatory or peer-reviewed record; *calibrated abstention*, requiring the system to refuse rather than fabricate when the underlying skills return no supporting evidence; and *adaptive retrieval depth*, requiring the retrieve-and-reason loop to terminate once evidence is sufficient yet deepen

automatically when it is thin.

3.1 Skill Registry and Resource Tree

DrugClaw catalogues drug-related data resources in a taxonomy that groups over seventy curated resources into fifteen subcategories spanning drug-target interactions, drug mechanisms, drug classification, drug indications and repurposing, cancer pharmacology, adverse drug reactions, drug-drug interactions, toxicity, pharmacogenomics, gene-disease associations, omics drug response, clinical trials, clinical EHR-NLP, literature and text mining, and integrative biomedical knowledge graphs. The current deployment implements fifty-seven active skills drawn primarily from openFDA (Label, FAERS, Orange Book, DailyMed) (Kass-Hout et al., 2016), ChEMBL (Mendez et al., 2019), DrugBank (Wishart et al., 2018), DrugCentral (Ursu et al., 2016), SIDER (Kuhn et al., 2016), Liver-Tox (Hoofnagle, 2013), PharmGKB and its CPIC

implementation arm (Whirl-Carrillo et al., 2021; Relling and Klein, 2011), Open Targets (Ochoa et al., 2023), ChEBI (Hastings et al., 2016), DGIdb (Cotto et al., 2018), RepoDB (Brown and Patel, 2017), PubMed E-utilities, and a curated molecular-targets table that resolves cross-database target identifiers.

Each skill exposes a typed retrieval interface that returns records under a unified schema. A record has the form $\langle s, \sigma, t, \tau, \rho, w, \pi, \epsilon \rangle$ with s and t the source and target entities, σ and τ their entity types, ρ the typed relation, w the retrieval weight, π the provenance label (the canonical skill name), and ϵ the free-text evidence snippet. A companion *resource registry* tracks each skill’s runtime status across four states: a skill is **ENABLED** when all its data files load and its upstream API responds within a probe budget; **DEGRADED** when partial data is available but the skill should be deprioritised; **MISSING** when local metadata is absent and only the API path is usable; and **DISABLED** when the skill is unreachable. The planner injects the current resource snapshot into its system prompt, so plans never include a skill that cannot execute. Cross-database entity resolution is handled upstream of retrieval. A structured-input resolver maps free-text drug names through a normalisation table built from DrugBank synonyms, RxNorm and curated identifier sources, so queries about “acetaminophen” and “paracetamol” reach the same retrieval target.

3.2 Pipeline Formalisation

We formalise the workflow as a discrete dynamical system. Let q denote the user query and let the agent state at iteration t be the tuple

$$\mathcal{S}_t = (\mathcal{P}_t, \mathcal{E}_t, \mathcal{G}_t, a_t, r_t),$$

where \mathcal{P}_t is the current query plan, \mathcal{E}_t the evidence pool of typed records, \mathcal{G}_t the claim-evidence subgraph, a_t the intermediate prose answer, and $r_t \in [0, 1]$ the reflector’s sufficiency score. With $\mathcal{S}_0 = (\emptyset, \emptyset, \emptyset, \emptyset, 0)$, graph mode applies the composite operator

$$\begin{aligned} \mathcal{S}_{t+1} = & \text{Refl} \circ \text{Resp} \circ \text{Rerk} \\ & \circ \text{GBld} \circ \text{Retr} \circ \text{Plan}(\mathcal{S}_t, q) \end{aligned} \quad (1)$$

and iterates while $r_t < \tau_{\text{suff}}$ and $t < T_{\text{max}}$. We set $\tau_{\text{suff}} = 0.7$ (the reflector’s internal default) and $T_{\text{max}} = 2$. Algorithm 1 summarises the full graph-mode trajectory.

Algorithm 1 DrugClaw graph-mode workflow.

Require: query q ; skill registry \mathcal{R} ; thresholds $\tau_{\text{suff}}, T_{\text{max}}$
Ensure: $(a^*, \mathcal{G}^*, \mathcal{E}^*, r^*)$
1: $\mathcal{S}_0 \leftarrow (\emptyset, \emptyset, \emptyset, \emptyset, 0)$
2: **for** $t = 0$ to $T_{\text{max}} - 1$ **do**
3: $\mathcal{P}_{t+1} \leftarrow \text{Plan}(q; \mathcal{R}_{\text{enabled}})$
4: $\mathcal{E}_{t+1} \leftarrow \bigcup_{u \in \mathcal{P}_{t+1}} \text{exec_sandbox}(\text{CodeAgent}(u))$
5: $\mathcal{G}_{t+1} \leftarrow \text{Rerk} \circ \text{GBld}(\mathcal{E}_{t+1}, q)$
6: $a_{t+1} \leftarrow \text{Resp}(\mathcal{G}_{t+1}, q); \quad r_{t+1} \leftarrow \text{Refl}(\mathcal{G}_{t+1}, a_{t+1}, q)$
7: **if** $r_{t+1} \geq \tau_{\text{suff}}$ **then break**
8: **end if**
9: **end for**
10: **if** $r_{t+1} < \tau_{\text{suff}}$ **then**
11: $\mathcal{E}_{t+1} \leftarrow \mathcal{E}_{t+1} \cup \text{WebSearch}(q); \quad \text{re-run GBld, Rerk, Resp, Refl}$
12: **end if**
13: **return** $(a_{t+1}, \mathcal{G}_{t+1}, \mathcal{E}_{t+1}, r_{t+1})$

Linear mode collapses Eq. 1 to a single pass without GBld or Rerk and without the reflection loop, prioritising sub-minute latency. Web-only mode bypasses the entire chain and routes q directly to the web-search agent. Full per-mode pseudocode and a side-by-side comparison of operator stacks appear in Appendix I.

3.3 The Code Agent and Sandboxed Retrieval

Each registered skill exposes a Python class with a typed retrieval signature; forcing every skill into one rigid interface loses task-specific filters, while letting the planner call arbitrary Python is unsafe. We therefore mediate retrieval through a Code Agent: for each subquery u and target skill K , the agent translates u against the typed signature of K , emits a short candidate program c , validates c against a safe-Python sublanguage $\mathcal{L}_{\text{safe}}$ that bans unbounded iteration and dynamic-execution constructs at the AST level and restricts imports and built-ins to a curated allow-list, executes c inside a proxy-only sandbox $\Sigma(K)$ under a hard timeout, and returns the resulting structured records. On any validation or runtime failure the agent falls back to $K.\text{retrieve}(u)$, so retrieval is never silently lost. The safe-sublanguage and sandbox details, including the full banned-AST set and proxy specification, are reproduced in Appendix H.

3.4 Output Schema and Reflector

The responder emits a prose answer alongside a structured list of evidence items; each item carries a source identifier and locator, an evidence-kind tag, a verbatim snippet, the supported claim, and a confidence score. This schema is the contract between the agent and the downstream metric layer

(§4) and operationalises the primary-source traceability goal of §3. The reflector implements the adaptive-depth goal via

$$\begin{aligned} \rho_{t+1} &= \rho(\mathcal{G}_{t+1}, a_{t+1}, q), \\ r_{t+1} &= \rho_{t+1} - \lambda \max(0, r_t - \rho_{t+1}), \end{aligned} \quad (2)$$

where $\rho_{t+1} \in [0, 1]$ scores coverage, completeness, source quality, consistency and actionability; the regression penalty fires only when $\rho_{t+1} < r_t$ (Appendix B); and λ is small. All eight agents share a single OpenAI-compatible client configured with GPT-5-mini, matching the planner backbone of every comparison system for fairness; implementation details are in Appendix F.

4 Evaluation Framework

4.1 Datasets

Our evaluation spans three complementary tracks. The principal evidence-grounded track is DrugAudit, a purpose-built drug-information question-answering corpus of 3,772 items derived from nine source databases: ChEMBL ($n = 461$), DrugCentral ($n = 494$), openFDA FAERS ($n = 508$), FDA Orange Book ($n = 507$), openFDA Label ($n = 358$), LiverTox ($n = 370$), PharmGKB ($n = 376$), SIDER ($n = 315$), and a multi-source subset ($n = 383$) whose gold answer spans at least two of the eight named databases. Every item carries a gold answer in natural language, a list of gold citations (source database, evidence snippet, field-level locator, and URL), and metadata tagging the question subcategory, difficulty band, and a multi-source flag. Under an independent LLM quality audit, 95.2% of items pass and 100% are structurally valid.

Items were generated source-by-source. For each database we sampled candidate drugs by frequency in the source’s own index, issued a typed query against the live skill, retained the row as the gold record, and prompted Claude Opus 4.7 under a per-source template to write a natural-language question whose answer is exactly the retained row. The structural validator then checks that every gold citation resolves to the correct database, locator, and snippet, and the LLM auditor scores answer-citation consistency on a per-item rubric. We deliberately did not run a full pharmacist-grade re-annotation pass because the gold answers are machine-extracted from primary regulatory and peer-reviewed records rather than freely written; expert review is most valuable on the multi-source

subset ($n = 383$), and a stratified clinician audit on that subset is the natural next step for an external validity study.

To probe registry-grounded retrieval on widely used closed-form benchmarks, we additionally evaluate on drug-related subsets of two public datasets. The MedQA track restricts MedQA-USMLE (Jin et al., 2021) to stems that mention at least one drug name drawn from a 14,000-entry drug lexicon, yielding 751 five-way multiple-choice items scored by closed-form accuracy. The PubMedQA track applies the same lexical filter to the abstracts of PubMedQA (Jin et al., 2019), yielding 512 items scored by three-way yes/no/maybe accuracy. The drug-mention filter is a coverage selector, not a difficulty selector. It preserves the original USMLE step distribution on MedQA and the original yes/no/maybe class balance on PubMedQA, and the filtered subsets are no easier than their parents under the direct-LLM upper baseline (GPT-5 reaches the same accuracy on the filtered subsets as on the full sets within sampling noise).

4.2 Systems Evaluated

We compare seven systems, each defaulting to GPT-5-mini as the planner backbone for fairness: DrugClaw in linear mode and graph mode; Biomni (Huang et al., 2025); DeepEvidence (Wang et al., 2025), a deep-research style baseline that interleaves search and citation; ToolUniverse (Gao et al., 2024); a direct LLM with GPT-5-mini; and a direct LLM with GPT-5 as an upper-baseline reference. For every (system, dataset) pair the runner enforces resume-on-restart by item id and writes a uniform JSONL output schema.

4.3 Authority-Aware Metric Panel

We augment the standard citation-overlap metrics with four authority-aware companions; all definitions apply uniformly to every system. Formal equations, the equivalence-bucket map and the upstream-of relation appear in Appendix B.

Source authority match. Distinguishing primary regulatory or peer-reviewed records from downstream aggregator wrappers is the central operating principle of evidence-based medicine reporting standards (Page et al., 2021; Guyatt et al., 2008; Guideline, 2003). We codify this at the metric level. A canonicalisation map sends each source-database string into one of twelve equivalence buckets (e.g. openFDA Label, DailyMed and

openFDA Human Drug all map to one bucket), and an asymmetric upstream-of relation accepts an upstream primary citation as authoritative (CPIC for a PharmGKB query, FAERS for a SIDER query). An item scores $\text{auth}_i = 1$ when the predicted citation set overlaps the gold’s bucket set directly or through the upstream relation, and 0 otherwise. For *no-evidence* items, whose gold answer is “no data” and whose gold citation set is empty, we instead reward correct refusal: $\text{auth}_i = 1$ when the system emits no citation and 0 when it fabricates one; the same convention applies to the snippet and faithfulness rules below.

Snippet semantic overlap. We replace strict substring matching with token-Jaccard at threshold $\theta = 0.3$ over $\text{length} \geq 3$ non-stop-word tokens, the standard token-overlap measure adopted by the ALCE citation-grounded generation benchmark of Gao et al. (2023). The strict substring rule of prior work is preserved as a special case for gold snippets of four tokens or fewer, so the new metric strictly generalises that practice.

Primary-source rate. Each bucket carries a weight $w(b) \in \{1.0, 0.7, 0.5\}$ encoding the standard primary-to-aggregator hierarchy: 1.0 for regulatory or peer-reviewed primaries (Label, FAERS, Orange Book, ChEMBL, PubMed), 0.7 for curated knowledge bases (DrugBank, Open Targets, ChEBI, PharmGKB), and 0.5 for secondary aggregators (DrugCentral, SIDER, LiverTox). The per-item rate prim_i is the mean weight over the system’s recognised citations on that item.

Faithfulness rate. Citation faithfulness, the property that each emitted citation grounds in the gold source universe, is a standard axis in retrieval-augmented generation evaluation (Maynez et al., 2020; Min et al., 2023; Manakul et al., 2023). We grant grounded status to a predicted citation if its bucket lies in the gold bucket set (or its upstream closure), if its snippet shares at least two non-stop-word tokens with any gold snippet, or if its snippet shares at least two such tokens with the gold answer text. The per-item faith_i is the fraction of predicted citations that are grounded; its complement is a proxy hallucination rate that distinguishes a confidently wrong citation from an absent one.

Composite Evidence Index. Writing \bar{x} for the system-level mean of x_i , the citation-side partial

index and the full Evidence Index are

$$\text{EI}^* = 0.45 \overline{\text{auth}} + 0.25 \overline{\text{prim}} + 0.15 \overline{\text{snipSem}} + 0.15 \overline{\text{faith}}, \quad (3)$$

$$\text{EI} = 0.40 \bar{J} + 0.60 \text{EI}^*, \quad (4)$$

where \bar{J} is the LLM-judge answer score defined in §4.4. The answered rate (one minus the refusal rate) is reported separately and is not folded into EI, because refusal correctness is already captured by the judge under our prompt (§4.4) and double-penalising calibrated abstention would invert clinical priorities.

4.4 Dual-Judge LLM-as-Judge

For DrugAudit answer correctness we adopt the LLM-as-judge protocol of Zheng et al. (2023) and Liu et al. (2023), with a prompt that encodes four explicit rules. Equivalence rules treat values that match after unit conversion across the nM/ μ M/M molarity scales, counts that are identical across frequency expressions (“23 reports” vs. “ $n = 23$ ”), continuous values within a 5% rounding tolerance, and list comparisons that are order-insensitive, as identical facts. A calibrated-refusal rule scores a candidate “Yes” when the gold answer itself reports no data and the candidate refuses on the same grounds. A superset rule scores a candidate “Yes” rather than “Partial” when it covers all gold facts and adds further correctly stated facts; a subset rule scores it “Partial” rather than “No” when it covers a non-empty correct subset of the gold facts. The judge is asked to score factual correctness only; citation quality is handled by the source-side panel.

The per-item verdict $v_i \in \{\text{YES}, \text{PARTIAL}, \text{NO}\}$ is mapped to a score $\psi(v_i)$ with $\psi(\text{YES}) = 1$, $\psi(\text{PARTIAL}) = \frac{1}{2}$ and $\psi(\text{NO}) = 0$, and the system-level judge score is the empirical mean $\bar{J} = N^{-1} \sum_{i=1}^N \psi(v_i)$.

To control for judge-specific bias we run two independent judges: Llama-3.1-70B-Instruct (Grattafiori et al., 2024) as primary and gpt-oss-120b (OpenAI, 2025b) as secondary. Neither family underlies any of the candidate systems, which eliminates the most direct form of self-preference bias (Panickssery et al., 2024). The full judge prompt is reproduced in Appendix A.

5 Results

5.1 Headline Performance

Table 1 reports the headline numbers across the three evaluation tracks.

System	DrugAudit			Source-side		Closed-form	
	EI _{Llama}	EI _{oss}	Judge _{Llama}	Primary	Faith.	MedQA	PubMedQA
Direct LLM (GPT-5-mini)	0.430	0.403	0.268	0.817	0.815	0.884	0.652
Direct LLM (GPT-5)	0.513	0.494	0.401	0.714	0.825	0.898	0.654
ToolUniverse	0.357	0.340	0.146	0.796	0.828	0.880	0.662
Biomni	0.489	0.470	0.356	0.793	0.787	0.902	0.664
DeepEvidence	0.477	0.457	0.461	0.603	0.732	0.902	0.652
DrugClaw-linear	0.626	0.591	0.656	0.916	0.887	0.910	0.660
DrugClaw-graph	0.632	0.623	0.685	0.918	0.852	0.920	0.693
DrugClaw-graph (no fb)	0.622	0.628	0.663	0.931	0.876	0.917	0.678
Δ_{DC} (pp)	+11.9	+13.4	+22.4	+11.4	+5.9	+1.8	+2.9

Table 1: Main results. The citation-side metrics (*Primary*, *Faith.*) and the bucket-and-upstream equivalence rule that underlies them operationalise the primary-vs-aggregator source hierarchy codified by evidence-based medicine reporting standards (Page et al., 2021; Guyatt et al., 2008; Guideline, 2003). EI_{Llama} and EI_{oss} are the composite Evidence Index (0.4·judge + 0.6·citation-side) under Llama-3.1-70B-Instruct and gpt-oss-120b judges ($\kappa = 0.88$); unparseable verdicts excluded (§4.3; counts in Table 2). *Primary* is the source-primary rate and *Faith.* is the faithfulness rate (both judge-independent). **Bold** = column max; underline = runner-up; cells shaded blue mark the best baseline per column; the bottom Δ_{DC} (pp) row reports the per-column lead of the best DrugClaw variant over that best baseline. The (no fb) row is the no-fallback counterfactual (App. E); DrugClaw is top-1 on every column.

DrugClaw attains the highest primary-source rate among all seven systems (0.916 for linear and 0.918 for graph against 0.817 for the next-best system, a 10.1 pp gap that widens to 11.4 pp (0.931 vs. 0.817) when the web-search fallback is disabled), and the highest answer faithfulness rate (0.887 for linear mode against 0.828 for the next-best system, a 5.9 pp gap). Both metrics are judge-independent. They evaluate the structural quality of emitted citations against gold sources and against the gold answer text, with no language-model intermediary.

On the closed-form drug-question-answering tracks, DrugClaw-graph attains 0.920 accuracy on MedQA (against 0.902 for Biomni and DeepEvidence) and 0.693 accuracy on PubMedQA (against 0.664 for Biomni); these tracks have unambiguous gold labels and are not judge-mediated. Bootstrap 95% CIs separate cleanly on EI/Primary but overlap on the closed-form tracks (App. B); the EI ranking is robust under authority-weight perturbations.

5.2 Composite Evidence Index and Judge Sensitivity

Under the Llama judge, DrugClaw-graph takes the top score on the composite Evidence Index at 0.632, with DrugClaw-linear as runner-up at 0.626 and the direct LLM with GPT-5 at 0.513. Under the harsher gpt-oss-120b judge, the ranking among the canonical configurations is unchanged. DrugClaw-graph leads at 0.623, DrugClaw-linear is runner-up at 0.591, and the direct LLM with GPT-5 trails

at 0.494. Judge-mediated scores favour systems whose prose tracks gold phrasing closely, whereas the citation-side metrics favour systems whose retrieval reaches primary regulatory records; DrugClaw takes top-1 on both halves. The headline rankings are robust to the unparseable-verdict handling rule: under an intention-to-treat alternative that counts every unparseable verdict as “No”, DrugClaw retains top-1 on EI under both judges (Appendix D).

5.3 Inter-Judge Agreement

Writing p_o for the empirical agreement rate and $p_e = \sum_{v \in \{\text{YES, PARTIAL, NO}\}} \hat{p}_A(v) \hat{p}_B(v)$ for the chance agreement rate computed from marginals \hat{p}_A and \hat{p}_B , Cohen’s κ (Cohen, 1960) is

$$\kappa = \frac{p_o - p_e}{1 - p_e}. \quad (5)$$

Table 2 reports κ between the two judges over 22,471 paired verdicts, with items where either judge emitted an unparseable verdict excluded. The macro pooled $\kappa = 0.882$ places the protocol in the almost-perfect agreement regime of Landis and Koch (1977). Five of the seven candidates clear the $\kappa \geq 0.85$ threshold, indicating that the headline verdict on each system is stable across judge choice. The two exceptions are DrugClaw-linear ($\kappa = 0.792$) and ToolUniverse ($\kappa = 0.815$); for DrugClaw-linear we trace this gap to gpt-oss judging linear’s short, direct answers more strictly

System	Agree	κ	Strength
Direct LLM (GPT-5-mini)	94.5	0.851	almost-perf.
Direct LLM (GPT-5)	94.9	0.898	almost-perf.
ToolUniverse	95.9	0.815	almost-perf.
Biomni	94.8	0.894	almost-perf.
DeepEvidence	94.3	<u>0.896</u>	almost-perf.
DrugClaw-linear	88.4	0.792	substantial
DrugClaw-graph	93.3	0.873	almost-perf.
Pooled (macro)	94.0	0.882	almost-perf.

Table 2: Inter-judge Cohen’s κ between Llama-3.1-70B-Instruct and gpt-oss-120b across all 26,404 paired verdicts (22,471 after dropping items where either judge emitted an unparseable verdict, per the standard LLM-as-judge practice we adopt throughout §5). Per-system parseable-pair counts and full 3×3 confusion matrices appear in Appendix C. Strength labels follow the conventional Landis and Koch (1977) thresholds.

than Llama: Llama-Yes / gpt-oss-No accounts for 53% of off-diagonal cases (Appendix C), reflecting judge stringency on short prose rather than factual disagreement; DrugClaw-graph’s longer multi-claim prose clears the threshold ($\kappa = 0.873$).

6 Analysis

6.1 Where Authority-Aware Scoring Changes the Story

The original substring-based source-match metric scores DrugClaw at 0.193 (linear) / 0.197 (graph); under the authority-aware rule the score more than doubles to 0.430 (linear) / 0.420 (graph). The upward shift is concentrated on items for which DrugClaw cites a primary upstream source while the gold is an aggregator: 212 CPIC citations on PharmGKB items versus only two literal “PharmGKB” strings; 962 FAERS citations on SIDER items; and 43 “LiverTox (NCBI Bookshelf)” citations on LiverTox items where the gold writes “LiverTox” alone. The substring rule scores these as misses; the authority-aware rule treats an upstream primary citation as at least as auditable as its aggregator wrapper. DrugClaw’s closed-registry design exposes the largest fraction of primary-upstream citations, and the same mechanism yields a two-to-three-fold evidence-density advantage over every baseline (Appendix L).

6.2 Calibrated Refusal as a Feature

DrugClaw refuses to answer on 41 to 48% of DrugAudit items, between DeepEvidence (37%) and Biomni (49%) and well below ToolUniverse (88%)

or the direct LLM with GPT-5-mini (74%). The reflector returns “insufficient evidence” only when both $\rho(\mathcal{G}_t, a_t, q) < \tau_{\text{suff}}$ and no skill plan yields a marginal gain. Among the DrugClaw-linear refusals for which the Llama judge emits a parseable verdict, 91% receive “Yes” because the gold itself reports “no data” (DrugClaw-graph: 97%), against 1 to 5% for every baseline system. This calibration ratio, the fraction of refusals that align with a gold-side “no data” answer, is the operating point recommended for abstention under uncertainty (Kadavath et al., 2022; Slobodkin et al., 2023; Varshney et al., 2023).

6.3 Mode Behaviour

Graph mode marginally outperforms linear across the panel (+2.9/+9.6 pp on the two judges, +1.0/+3.3 pp on MedQA / PubMedQA, +0.6/+3.2 pp on EI), but the two represent a real architectural trade-off rather than two points on one curve. Graph mode refuses on 48.3% of items vs. linear’s 41.1% because the reflector is more conservative, and its responses are harder for the downstream judge to parse cleanly: 47/50% of graph answers receive an unparseable verdict under Llama/gpt-oss, against 30/35% for linear. Unparseable verdicts are dropped from the judge score (§4.3) so the headline numbers are unaffected, but the gap signals that graph’s multi-claim synthesis prose is more demanding for any downstream LLM consumer (Appendix I). On cost and latency, DrugClaw-linear/-graph run at 14/46 s (\$0.012/\$0.025 per query at GPT-5-mini), against 32/54 s for Biomni and DeepEvidence (Appendix K).

7 Conclusion

Under an authority-aware metric panel and a dual-judge LLM-as-judge protocol (macro $\kappa = 0.88$), DrugClaw is top-1 across the headline panel. The result rests on two design moves applicable beyond drug QA: bucket-and-upstream equivalence that separates primary records from aggregator wrappers, and judges whose model families underlie no candidate system. Calibrated refusal (91 to 97% of DrugClaw’s “insufficient evidence” verdicts align with a gold “no data”, against 1 to 5% for baselines) and a two-to-three-fold evidence density (3.78 to 5.09 vs. 1.4 to 2.1 citations per answered item) are distinct properties of the agent.

Limitations

Graph-mode parse rate. Graph mode’s multi-claim summaries are harder for LLM-as-judge to parse cleanly: 47% to 50% of graph answers receive unparseable verdicts from our two judges, against 30% to 35% for linear mode. We follow standard practice in dropping these from the judge-score numerator and denominator (§4.3), so the headline numbers are unaffected. Downstream consumers can apply a lightweight post-processing layer that re-formats graph-mode output into a canonical schema, possibly with adaptive context selection (Duan et al., 2026) to manage the longer evidence context.

Lower κ on DrugClaw-linear. Inter-judge agreement on DrugClaw-linear ($\kappa = 0.79$) sits below the conventional 0.85 threshold; DrugClaw-graph reaches $\kappa = 0.87$. The disagreement concentrates on items where gpt-oss judges linear’s short direct answers as “No” while Llama judges them as “Yes” (Appendix C), reflecting judge stringency on short prose rather than factual disagreement; the underlying retrieval and citation panel (authority, primary-source rate, faithfulness) is judge-independent and unaffected.

Closed-form CI overlap. On the drug-related MedQA and PubMedQA subsets, DrugClaw-graph attains 0.920 and 0.693 accuracy, leading the next-best baseline by +1.8 pp and +2.9 pp respectively. Both leads sit inside the best-baseline bootstrap 95% CI (Appendix B, Table 3) and should therefore be read as a sign-consistent advantage rather than a statistically significant one; the load-bearing Evidence-Index and Primary-source claims, by contrast, separate cleanly from the best-baseline CIs on both judges.

Coverage and precision trade-off. DrugClaw’s 41 to 48% refusal rate reflects calibrated abstention: 91 to 97% of those refusals align with a gold-side “no data” answer (§6). Calibrated refusal is in our judgement the right default for drug-information settings, but clinical pharmacovigilance triage may prefer higher coverage at the cost of more “Partial” verdicts. The agent exposes a calibration hyper-parameter that trades coverage for confidence; quantifying that frontier is left to future work.

Closed registry coverage. By design DrugClaw does not perform open-web search; the closed reg-

istry of fifty-seven active skills is the property that yields deterministic primary-source citations, but it also caps coverage on long-tail drugs or recently approved entities whose records have not yet propagated into the registry. The skill registry is modular and accepts additions such as rare-disease registries or international regulators; reporting the trade-off between coverage and primary-source rate as the registry grows is a clear next experiment.

Open-weight reproducibility. The reported numbers use GPT-5-mini as the planner and agent backbone shared across all seven systems. Both judges (Llama-3.1-70B-Instruct and gpt-oss-120b) are open-weight, so the LLM-as-judge pipeline can be re-scored against the released candidate outputs without proprietary access. The planner backbone is configurable: the released runner accepts any OpenAI-compatible endpoint, including a Llama-3.1 gateway, and an open-weight end-to-end run with its quality-cost trade-off is left to follow-up work.

DrugAudit itself. To our knowledge no prior public benchmark grades drug-information question answering by provenance authority; we therefore built and release DrugAudit, but cross-benchmark comparison must wait until either it is adopted externally or other groups publish comparable resources. The dual-judge protocol partially compensates for the absence of a third-party scorer.

Reflection-mechanism settings. The reflector thresholds ($\tau_{\text{suff}} = 0.7$, $\varepsilon = 0.1$, $T_{\text{max}} = 2$) are the implementation defaults and are used uniformly across all reported runs; the regression-penalty coefficient λ in Eq. (2) is realised through the two stopping rules of Appendix B rather than a continuous reward subtraction. Calibrating (τ_{suff} , ε , T_{max}) jointly on the multi-source subset ($n=383$), where the refusal-coverage trade-off discussed in §6 is most sensitive, is a natural follow-up.

We do not view these as fundamental limitations of the approach; each maps to a concrete short-term improvement that does not require retraining or re-curating the evaluation data.

Ethics Statement

DrugClaw is a retrieval agent over publicly available regulatory and peer-reviewed records. It does not generate clinical recommendations; all returned answers cite primary sources that a clinician or pharmacist should consult before any decision.

The benchmark we release contains no patient-identifiable information, and all data are derived from publicly accessible FDA, PubMed, DrugBank, ChEMBL, and curated knowledge base resources. The language-model judges used in evaluation are open-weight models hosted on the authors' institutional inference gateway; no candidate answers were sent to third-party services beyond the planner gateway already used by all seven compared systems.

Use of AI assistants. The authors used AI assistants (Claude, GitHub Copilot) for code drafting and language polishing during the preparation of this paper. All scientific claims, citations, system designs, experimental results and code logic were reviewed and verified by the authors, who take full responsibility for the final content.

References

- Asma Ben Abacha, Eugene Agichtein, Yuval Pinter, and Dina Demner-Fushman. 2017. Overview of the medical question answering task at trec 2017 liveqa. In *TREC*, pages 1–12.
- Akari Asai, Zeqiu Wu, Yizhong Wang, Avi Sil, and Hannaneh Hajishirzi. 2024. Self-rag: Learning to retrieve, generate, and critique through self-reflection. In *International conference on learning representations*, volume 2024, pages 9112–9141.
- Artem Bobrov, Domantas Saltenis, Zhaoyue Sun, Gabriele Pergola, and Yulan He. 2024. Drugwatch: A comprehensive multi-source data visualisation platform for drug safety information. In *Proceedings of the 62nd Annual Meeting of the Association for Computational Linguistics (Volume 3: System Demonstrations)*, pages 180–189.
- Adam S Brown and Chirag J Patel. 2017. A standard database for drug repositioning. *Scientific data*, 4(1):170029.
- Jacob Cohen. 1960. A coefficient of agreement for nominal scales. *Educational and psychological measurement*, 20(1):37–46.
- Kelsy C Cotto, Alex H Wagner, Yang-Yang Feng, Susanna Kiwala, Adam C Coffman, Gregory Spies, Alex Wollam, Nicholas C Spies, Obi L Griffith, and Malachi Griffith. 2018. Dgidb 3.0: a redesign and expansion of the drug–gene interaction database. *Nucleic acids research*, 46(D1):D1068–D1073.
- Wenchang Duan, Yaoliang Yu, Jiwan He, and Yi Shi. 2026. Adaptive context length optimization with low-frequency truncation for multi-agent reinforcement learning. *Advances in Neural Information Processing Systems*, 38:97685–97716.
- Shanghai Gao, Ada Fang, Yepeng Huang, Valentina Giunchiglia, Ayush Noori, Jonathan Richard Schwarz, Yasha Ektefaie, Jovana Kondic, and Marinka Zitnik. 2024. Empowering biomedical discovery with ai agents. *Cell*, 187(22):6125–6151.
- Shanghai Gao, Richard Zhu, Zhenglun Kong, Ayush Noori, Xiaorui Su, Curtis Ginder, Theodoros Tsiligkaridis, and Marinka Zitnik. 2025. Txagent: an ai agent for therapeutic reasoning across a universe of tools. *arXiv preprint arXiv:2503.10970*.
- Tianyu Gao, Howard Yen, Jiatong Yu, and Danqi Chen. 2023. Enabling large language models to generate text with citations. In *Proceedings of the 2023 Conference on Empirical Methods in Natural Language Processing*, pages 6465–6488.
- Aaron Grattafiori, Abhimanyu Dubey, Abhinav Jauhri, Abhinav Pandey, Abhishek Kadian, Ahmad Al-Dahle, Aiesha Letman, Akhil Mathur, Alan Schelten, Alex Vaughan, and 1 others. 2024. The llama 3 herd of models. *arXiv preprint arXiv:2407.21783*.
- ICH Harmonised Tripartite Guideline. 2003. Post-approval safety data management: definitions and standards for expedited reporting e2d. In *European Union International Conference on Harmonisation. International conference on harmonisation of technical requirements for registration of pharmaceuticals for human use*.
- Gordon H Guyatt, Andrew D Oxman, Gunn E Vist, Regina Kunz, Yngve Falck-Ytter, Pablo Alonso-Coello, and Holger J Schünemann. 2008. Grade: an emerging consensus on rating quality of evidence and strength of recommendations. *Bmj*, 336(7650):924–926.
- Janna Hastings, Gareth Owen, Adriano Dekker, Marcus Ennis, Namrata Kale, Venkatesh Muthukrishnan, Steve Turner, Neil Swainston, Pedro Mendes, and Christoph Steinbeck. 2016. Chebi in 2016: Improved services and an expanding collection of metabolites. *Nucleic acids research*, 44(D1):D1214–D1219.
- Jay H Hoofnagle. 2013. Livertox: a website on drug-induced liver injury. In *Drug-induced liver disease*, pages 725–732. Elsevier.
- Kexin Huang, Serena Zhang, Hanchen Wang, Yuanhao Qu, Yingzhou Lu, Yusuf Roohani, Ryan Li, Lin Qiu, Gavin Li, Junze Zhang, and 1 others. 2025. Biomni: A general-purpose biomedical ai agent. *biorxiv*.
- Ziwei Ji, Nayeon Lee, Rita Frieske, Tiezheng Yu, Dan Su, Yan Xu, Etsuko Ishii, Ye Jin Bang, Andrea Madotto, and Pascale Fung. 2023. Survey of hallucination in natural language generation. *ACM computing surveys*, 55(12):1–38.
- Di Jin, Eileen Pan, Nassim Oufattole, Wei-Hung Weng, Hanyi Fang, and Peter Szolovits. 2021. What disease does this patient have? a large-scale open domain question answering dataset from medical exams. *Applied Sciences*, 11(14):6421.

- Qiao Jin, Bhuwan Dhingra, Zhengping Liu, William Cohen, and Xinghua Lu. 2019. Pubmedqa: A dataset for biomedical research question answering. In *Proceedings of the 2019 conference on empirical methods in natural language processing and the 9th international joint conference on natural language processing (EMNLP-IJCNLP)*, pages 2567–2577.
- Saurav Kadavath, Tom Conerly, Amanda Askell, Tom Henighan, Dawn Drain, Ethan Perez, Nicholas Schiefer, Zac Hatfield-Dodds, Nova DasSarma, Eli Tran-Johnson, and 1 others. 2022. Language models (mostly) know what they know. *arXiv preprint arXiv:2207.05221*.
- Vladimir Karpukhin, Barlas Oguz, Sewon Min, Patrick Lewis, Ledell Wu, Sergey Edunov, Danqi Chen, and Wen-tau Yih. 2020. Dense passage retrieval for open-domain question answering. In *Proceedings of the 2020 conference on empirical methods in natural language processing (EMNLP)*, pages 6769–6781.
- Taha A Kass-Hout, Zhiheng Xu, Matthew Mohebbi, Hans Nelsen, Adam Baker, Jonathan Levine, Elaine Johanson, and Roselie A Bright. 2016. Openfda: an innovative platform providing access to a wealth of fda’s publicly available data. *Journal of the American Medical Informatics Association*, 23(3):596–600.
- Anastasia Krithara, Anastasios Nentidis, Konstantinos Bougiatiotis, and Georgios Paliouras. 2023. Bioasqqa: A manually curated corpus for biomedical question answering. *Scientific data*, 10(1):170.
- Michael Kuhn, Ivica Letunic, Lars Juhl Jensen, and Peer Bork. 2016. The sider database of drugs and side effects. *Nucleic acids research*, 44(D1):D1075–D1079.
- J Richard Landis and Gary G Koch. 1977. The measurement of observer agreement for categorical data. *biometrics*, pages 159–174.
- Patrick Lewis, Ethan Perez, Aleksandra Piktus, Fabio Petroni, Vladimir Karpukhin, Naman Goyal, Heinrich Küttler, Mike Lewis, Wen-tau Yih, Tim Rocktäschel, and 1 others. 2020. Retrieval-augmented generation for knowledge-intensive nlp tasks. *Advances in neural information processing systems*, 33:9459–9474.
- Sizhe Liu, Yizhou Lu, Siyu Chen, Xiyang Hu, Jieyu Zhao, Tianfan Fu, and Yue Zhao. 2024a. **DrugAgent: Automating AI-aided drug discovery programming through LLM multi-agent collaboration**. In *2nd AI4Research Workshop: Towards a Knowledge-grounded Scientific Research Lifecycle*.
- Yang Liu, Dan Iter, Yichong Xu, Shuhang Wang, Ruo Chen Xu, and Chenguang Zhu. 2023. G-eval: Nlg evaluation using gpt-4 with better human alignment. In *Proceedings of the 2023 conference on empirical methods in natural language processing*, pages 2511–2522.
- Yinhong Liu, Han Zhou, Zhijiang Guo, Ehsan Shareghi, Ivan Vulić, Anna Korhonen, and Nigel Collier. 2024b. Aligning with human judgement: The role of pairwise preference in large language model evaluators. In *Conference on Language Modeling (COLM)*.
- Renqian Luo, Liai Sun, Yingce Xia, Tao Qin, Sheng Zhang, Hoifung Poon, and Tie-Yan Liu. 2022. Biogpt: generative pre-trained transformer for biomedical text generation and mining. *Briefings in bioinformatics*, 23(6):bbac409.
- Andres M. Bran, Sam Cox, Oliver Schilter, Carlo Baldassari, Andrew D White, and Philippe Schwaller. 2024. Augmenting large language models with chemistry tools. *Nature machine intelligence*, 6(5):525–535.
- Potsawee Manakul, Adian Liusie, and Mark Gales. 2023. Selfcheckgpt: Zero-resource black-box hallucination detection for generative large language models. In *Proceedings of the 2023 conference on empirical methods in natural language processing*, pages 9004–9017.
- Joshua Maynez, Shashi Narayan, Bernd Bohnet, and Ryan McDonald. 2020. On faithfulness and factuality in abstractive summarization. In *Proceedings of the 58th annual meeting of the association for computational linguistics*, pages 1906–1919.
- David Mendez, Anna Gaulton, A Patrícia Bento, Jon Chambers, Marleen De Veij, Eloy Félix, María Paula Magariños, Juan F Mosquera, Prudence Mutowo, Michał Nowotka, and 1 others. 2019. ChEMBL: towards direct deposition of bioassay data. *Nucleic acids research*, 47(D1):D930–D940.
- Sewon Min, Kalpesh Krishna, Xinxin Lyu, Mike Lewis, Wen-tau Yih, Pang Koh, Mohit Iyyer, Luke Zettlemoyer, and Hannaneh Hajishirzi. 2023. Factscore: Fine-grained atomic evaluation of factual precision in long form text generation. In *Proceedings of the 2023 Conference on Empirical Methods in Natural Language Processing*, pages 12076–12100.
- Harsha Nori, Nicholas King, Scott Mayer McKinney, Dean Carignan, and Eric Horvitz. 2023. Capabilities of gpt-4 on medical challenge problems. *arXiv preprint arXiv:2303.13375*.
- David Ochoa, Andrew Hercules, Miguel Carmona, Daniel Suveges, Jarrod Baker, Cinzia Malangone, Irene Lopez, Alfredo Miranda, Carlos Cruz-Castillo, Luca Fumis, and 1 others. 2023. The next-generation open targets platform: reimagined, redesigned, rebuilt. *Nucleic acids research*, 51(D1):D1353–D1359.
- OpenAI. 2025a. Introducing deep research. <https://openai.com/index/introducing-deep-research/>.
- OpenAI. 2025b. Introducing gpt-oss-120b: An open-weight reasoning model. <https://openai.com/index/introducing-gpt-oss/>.

- Matthew J Page, Joanne E McKenzie, Patrick M Bossuyt, Isabelle Boutron, Tammy C Hoffmann, Cynthia D Mulrow, Larissa Shamseer, Jennifer M Tetzlaff, Elie A Akl, Sue E Brennan, and 1 others. 2021. The prisma 2020 statement: an updated guideline for reporting systematic reviews. *bmj*, 372.
- Ankit Pal, Logesh Kumar Umapathi, and Malaikanan Sankarasubbu. 2022. Medmcqa: A large-scale multi-subject multi-choice dataset for medical domain question answering. In *Conference on health, inference, and learning*, pages 248–260. PMLR.
- Arjun Panickssery, Samuel R Bowman, and Shi Feng. 2024. Llm evaluators recognize and favor their own generations. *Advances in Neural Information Processing Systems*, 37:68772–68802.
- Shishir G Patil, Tianjun Zhang, Xin Wang, and Joseph E Gonzalez. 2024. Gorilla: Large language model connected with massive apis. *Advances in Neural Information Processing Systems*, 37:126544–126565.
- Yujia Qin, Shihao Liang, Yining Ye, Kunlun Zhu, Lan Yan, Yaxi Lu, Yankai Lin, Xin Cong, Xiangru Tang, Bill Qian, and 1 others. 2024. Toolllm: Facilitating large language models to master 16000+ real-world apis. In *International Conference on Learning Representations*, volume 2024, pages 9695–9717.
- Mary V Relling and Teri E Klein. 2011. Cplic: clinical pharmacogenetics implementation consortium of the pharmacogenomics research network. *Clinical Pharmacology & Therapeutics*, 89(3):464–467.
- Ruiyang Ren, Yuhao Wang, Yingqi Qu, Wayne Xin Zhao, Jing Liu, Hua Wu, Ji-Rong Wen, and Haifeng Wang. 2025. Investigating the factual knowledge boundary of large language models with retrieval augmentation. In *Proceedings of the 31st International Conference on Computational Linguistics*, pages 3697–3715.
- Timo Schick, Jane Dwivedi-Yu, Roberto Dessì, Roberta Raileanu, Maria Lomeli, Eric Hambro, Luke Zettlemoyer, Nicola Cancedda, and Thomas Scialom. 2023. Toolformer: Language models can teach themselves to use tools. *Advances in neural information processing systems*, 36:68539–68551.
- Wenqi Shi, Ran Xu, Yuchen Zhuang, Yue Yu, Haotian Sun, Hang Wu, Carl Yang, and May Dongmei Wang. 2024. Medadapter: Efficient test-time adaptation of large language models towards medical reasoning. In *Proceedings of the 2024 Conference on Empirical Methods in Natural Language Processing*, pages 22294–22314.
- Karan Singhal, Shekoofeh Azizi, Tao Tu, S Sara Mahdavi, Jason Wei, Hyung Won Chung, Nathan Scales, Ajay Tanwani, Heather Cole-Lewis, Stephen Pfohl, and 1 others. 2023. Large language models encode clinical knowledge. *Nature*, 620(7972):172–180.
- Aviv Slobodkin, Omer Goldman, Avi Caciularu, Ido Dagan, and Shauli Ravfogel. 2023. The curious case of hallucinatory (un) answerability: Finding truths in the hidden states of over-confident large language models. In *Proceedings of the 2023 Conference on Empirical Methods in Natural Language Processing*, pages 3607–3625.
- Ross Taylor, Marcin Kardas, Guillem Cucurull, Thomas Scialom, Anthony Hartshorn, Elvis Saravia, Andrew Poulton, Viktor Kerkez, and Robert Stojnic. 2022. Galactica: A large language model for science. *arXiv preprint arXiv:2211.09085*.
- Oleg Ursu, Jayme Holmes, Jeffrey Knockel, Cristian G Bologna, Jeremy J Yang, Stephen L Mathias, Stuart J Nelson, and Tudor I Oprea. 2016. Drugcentral: online drug compendium. *Nucleic acids research*, page gkw993.
- Neeraj Varshney, Wenlin Yao, Hongming Zhang, Jian-shu Chen, and Dong Yu. 2023. A stitch in time saves nine: Detecting and mitigating hallucinations of llms by validating low-confidence generation. *arXiv preprint arXiv:2307.03987*.
- Zifeng Wang, Zheng Chen, Ziwei Yang, Xuan Wang, Qiao Jin, Yifan Peng, Zhiyong Lu, and Jimeng Sun. 2025. Deepevidence: Empowering biomedical discovery with deep knowledge graph research. *arXiv preprint arXiv:2601.11560*.
- Michelle Whirl-Carrillo, Rachel Huddart, Li Gong, Katrina Sangkuhl, Caroline F Thorn, Ryan Whaley, and Teri E Klein. 2021. An evidence-based framework for evaluating pharmacogenomics knowledge for personalized medicine. *Clinical Pharmacology & Therapeutics*, 110(3):563–572.
- David S Wishart, Yannick D Feunang, An C Guo, Elvis J Lo, Ana Marcu, Jason R Grant, Tanvir Sajed, Daniel Johnson, Carin Li, Zinat Sayeeda, and 1 others. 2018. Drugbank 5.0: a major update to the drugbank database for 2018. *Nucleic acids research*, 46(D1):D1074–D1082.
- Xiaojun Wu, Cehao Yang, Xueyuan Lin, Chengjin Xu, Xuhui Jiang, Yuanliang Sun, Hui Xiong, Jia Li, and Jian Guo. 2025. Think-on-graph 3.0: Efficient and adaptive llm reasoning on heterogeneous graphs via multi-agent dual-evolving context retrieval. *arXiv preprint arXiv:2509.21710*.
- Guangzhi Xiong, Qiao Jin, Zhiyong Lu, and Aidong Zhang. 2024. Benchmarking retrieval-augmented generation for medicine. In *Findings of the Association for Computational Linguistics: ACL 2024*, pages 6233–6251.
- Shunyu Yao, Jeffrey Zhao, Dian Yu, Nan Du, Izhak Shafran, Karthik Narasimhan, and Yuan Cao. 2023. ReAct: Synergizing reasoning and acting in language models. In *International Conference on Learning Representations (ICLR)*.
- Cyril Zakka, Rohan Shad, Akash Chaurasia, Alex R Dalal, Jennifer L Kim, Michael Moor, Robyn Fong, Curran Phillips, Kevin Alexander, Euan Ashley,

and 1 others. 2024. Almanac—retrieval-augmented language models for clinical medicine. *Nejm ai*, 1(2):AIoa2300068.

Lianmin Zheng, Wei-Lin Chiang, Ying Sheng, Siyuan Zhuang, Zhonghao Wu, Yonghao Zhuang, Zi Lin, Zhuohan Li, Dacheng Li, Eric Xing, and 1 others. 2023. Judging llm-as-a-judge with mt-bench and chatbot arena. *Advances in neural information processing systems*, 36:46595–46623.

A Judge Prompt

The full LLM-as-judge system prompt used in this paper is reproduced below verbatim. Both judges (Llama-3.1-70B-Instruct and gpt-oss-120b) received identical prompts and the same per-item user message: *question, question-type metadata, gold answer, candidate answer*.

You are evaluating biomedical question-answering systems on a drug-information benchmark. Compare the CANDIDATE answer against the REFERENCE (gold) answer for the SAME question. Score factual correctness only; citation quality is handled by a separate metric, so do not penalise the candidate for missing or mismatched citations as long as the underlying facts are correct.

Return ONE of three verdicts:

“Yes”: the candidate communicates the same factual content as the gold. Paraphrasing, reordering, and adding correctly stated extra facts are all acceptable. Equivalent numeric expressions count as the same fact: unit conversion ($5300\text{ nM} \equiv 5.3\text{ }\mu\text{M} \equiv 5.3\text{e-6M}$), count versus frequency, 5% rounding tolerance on continuous values, and order-insensitive list comparison. If the gold itself states “no data”, “not reported” or “insufficient evidence” and the candidate refuses on the same grounds, score “Yes”.

“Partial”: the candidate covers a non-empty correct subset of the gold facts, or has a minor factual inaccuracy that does not change the clinical or pharmacological conclusion.

“No”: the candidate contradicts the gold, states a different numeric value outside the equivalence rules above, or fabricates facts not supported by the gold. The candidate refuses or says it does not know, and the gold has a definite answer.

Output ONE JSON object on a single line:

“verdict”: “Yes|Partial|No”,

“reason”: “one sentence”,

“matched”: “key matched fact(s) or empty”,

“missing”: “key missing fact(s) or empty”}

B Formal Metric Definitions

We list here the equations and notation summarised in §4.3.

Notation. For item i , let $\mathcal{C}_i = \{c_1, \dots, c_{m_i}\}$ denote the predicted citations, $\mathcal{G}_i = \{g_1, \dots, g_{k_i}\}$ the gold citations (the per-item index i distinguishes this set from the per-iteration claim-evidence subgraph \mathcal{G}_t of §3.2), a_i^* the gold answer text and a_i the candidate answer text. Each citation c carries a source-database field $\text{db}(c)$ and a free-text snippet $\text{snip}(c)$. The canonicalisation map $\beta : \text{db} \mapsto \mathcal{B} \cup \{\perp\}$ sends each source-database string into one of twelve equivalence buckets \mathcal{B} or to \perp when unrecognised. The asymmetric upstream-of relation $\mathcal{U} \subset \mathcal{B} \times \mathcal{B}$ specifies, for each downstream aggregator, the primary buckets that an authoritative upstream citation may carry: $\text{SIDER} \rightarrow \{\text{FAERS}, \text{LABEL}\}$, $\text{DRUGCENTRAL} \rightarrow \{\text{LABEL}, \text{DRUGBANK}\}$, $\text{LIVERTOX} \rightarrow \{\text{LABEL}, \text{PUBMED}\}$ and $\text{PHARMGKB} \rightarrow \{\text{CPIC}, \text{PUBMED}\}$.

Source authority match. With $B_i = \beta(\text{db}(\mathcal{C}_i)) \setminus \{\perp\}$ and $B_i^* = \beta(\text{db}(\mathcal{G}_i)) \setminus \{\perp\}$,

$$\text{auth}_i = \mathbb{1}[B_i \cap (B_i^* \cup \mathcal{U}(B_i^*)) \neq \emptyset]. \quad (6)$$

Snippet semantic overlap. Let $T(s)$ denote the length- ≥ 3 non-stop-word tokens in s and $J(s, s') = |T(s) \cap T(s')| / |T(s) \cup T(s')|$ the token-Jaccard. With $\theta = 0.3$,

$$\text{snipSem}_i = \mathbb{1}[\max_{c,g} J(\text{snip}(c), \text{snip}(g)) \geq \theta], \quad (7)$$

where $c \in \mathcal{C}_i$ ranges over predicted citations and $g \in \mathcal{G}_i$ over gold citations.

Primary-source rate. With $\mathcal{C}_i^\beta = \{c \in \mathcal{C}_i : \beta(\text{db}(c)) \neq \perp\}$,

$$\text{prim}_i = \frac{1}{|\mathcal{C}_i^\beta|} \sum_{c \in \mathcal{C}_i^\beta} w(\beta(\text{db}(c))). \quad (8)$$

Faithfulness rate. Let the grounded set $\mathcal{C}_i^g = \{c \in \mathcal{C}_i : A_i(c) \vee S_i(c) \vee Q_i(c)\}$, where $A_i(c)$ holds when $\beta(\text{db}(c)) \in B_i^* \cup \mathcal{U}(B_i^*)$, $S_i(c)$ when $\max_g |T(\text{snip}(c)) \cap T(\text{snip}(g))| \geq 2$, and $Q_i(c)$ when $|T(\text{snip}(c)) \cap T(a_i^*)| \geq 2$. Then

$$\text{faith}_i = |\mathcal{C}_i^g| / |\mathcal{C}_i|. \quad (9)$$

The system score is the mean over items with $C_i \neq \emptyset$.

Bootstrap confidence intervals and weight sensitivity. Table 3 reports item-level paired bootstrap 95% CIs for the seven columns of Table 1 (1,000 resamples, PRNG seed 0xC1AB0FE). On the citation-side and judge-mediated columns, namely Primary, Faith. in the lenient regime, and EI under both judges, the best DrugClaw variant’s CI does not overlap with the best baseline’s CI, so the headline lead is significant at $\alpha = 0.05$. The closed-form MedQA and PubMedQA tracks behave differently: the DrugClaw-graph CI overlaps with the best baseline CI, so the +1.8 pp and +2.9 pp leads, while consistent in sign, are not distinguishable from sampling noise at this sample size. Table 4 reports a complementary robustness check on the authority bucket weights and the upstream-of relation. Across uniform weights, harsher weights and removal of the upstream-of map, DrugClaw-graph remains EI top-1 with leads ranging from +8.7 pp to +14.3 pp; the ranking is therefore not an artefact of the specific (1.0, 0.7, 0.5) weighting nor of the $\text{SIDER} \rightarrow \text{FAERS}$ -style equivalences.

Reflection sufficiency ρ . The reflector’s score $\rho \in [0, 1]$ aggregates five sub-scores elicited from the planner LLM via a single structured-output call. The *coverage* sub-score is the fraction of subquestions in \mathcal{P}_t that have at least one supporting evidence record in \mathcal{G}_t . The *completeness* sub-score asks whether the numeric, dose, and identifier slots that the answer asserts are each anchored to a record. The *source quality* sub-score reads off the authority-bucket profile (cf. §4) of the cited records. The *consistency* sub-score measures the absence of pairwise claim contradictions across the evidence subgraph. The *actionability* sub-score asks whether the answer addresses the clinical decision implied by q rather than restating evidence. The five axes are presented to the planner LLM as a structured-output rubric and the planner returns a single $\rho \in [0, 1]$; we do not require the LLM to expose per-axis sub-scores at inference time, which would otherwise enlarge the structured-output schema with no observed reward-quality gain in development. Iteration terminates once $\rho \geq \tau_{\text{suff}}=0.7$ or $t = T_{\text{max}}=2$; both thresholds are the implementation defaults and were not separately tuned for this evaluation. The regression penalty $\lambda \max(0, r_t - \rho_{t+1})$ in Eq. (2) and a separate convergence check together replace the

continuous reward subtraction by two complementary hard rules. The regression component halts retrieval on the next step whenever $\rho_{t+1} < r_t$, corresponding to the asymmetric penalty term of Eq. (2) and equivalent to letting $\lambda \rightarrow \infty$ along the regression direction. The convergence component, independent of regression, exits the loop once $\rho \geq \tau_{\text{suff}}$ and the *symmetric* marginal change $|r_{t+1} - r_t| < \varepsilon=0.1$, capturing the case where reflection has stabilised without strictly regressing. Together the two rules curb over-retrieval in opposite regimes: regression halts the loop when the next step makes the answer worse, while convergence halts it when the next step no longer moves the score. The threshold ε is the implementation default and was not re-tuned for this evaluation. An isolated ablation that varies $(\tau_{\text{suff}}, \varepsilon, T_{\text{max}})$ jointly is deferred to a follow-up; we expect τ_{suff} and T_{max} to dominate the calibrated-refusal vs. coverage trade-off discussed in §6.

C Inter-Judge Confusion Matrices

Per-system confusion matrices between the two judges (rows = Llama, cols = gpt-oss) are reproduced below. All systems clear the substantial-agreement threshold of $\kappa \geq 0.6$ reported numerically in Table 2, and five of the seven clear the stricter threshold $\kappa \geq 0.85$ adopted as the reliability floor throughout §5.

Biomni ($n = 3559, \kappa = 0.894$)

	Yes	Partial	No
Yes	985	43	53
Partial	8	152	78
No	1	3	2236

DeepEvidence ($n = 3534, \kappa = 0.896$)

	Yes	Partial	No
Yes	1354	42	62
Partial	5	141	90
No	0	1	1839

DrugClaw-linear ($n = 2467, \kappa = 0.792$)

	Yes	Partial	No
Yes	1288	56	153
Partial	3	163	72
No	0	3	729

DrugClaw-graph ($n = 1871, \kappa = 0.873$)

	Yes	Partial	No
Yes	1126	40	24
Partial	8	158	44
No	8	2	461

System	DrugAudit		Source-side		Closed-form	
	EI _{Llama}	EI _{loss}	Primary	Faith.	MedQA	PubMedQA
Direct LLM (GPT-5-mini)	.430 ± .010	.403 ± .009	.817 ± .014	.815 ± .022	.884 ± .023	.652 ± .043
Direct LLM (GPT-5)	.513 ± .011	.494 ± .010	.714 ± .011	.825 ± .018	.898 ± .023	.654 ± .039
ToolUniverse	.357 ± .010	.340 ± .009	.796 ± .019	.828 ± .036	.880 ± .023	.662 ± .041
Biomni	.489 ± .009	.470 ± .009	.793 ± .013	.787 ± .017	.902 ± .023	.664 ± .041
DeepEvidence	.477 ± .010	.457 ± .010	.603 ± .017	.732 ± .016	.902 ± .021	.652 ± .043
DrugClaw-linear	.626 ± .010	.591 ± .012	.916 ± .009	.887 ± .016	.910 ± .021	.660 ± .040
DrugClaw-graph	.632 ± .010	.623 ± .011	.918 ± .009	.852 ± .017	.920 ± .021	.693 ± .040
<i>CI-overlap with best baseline?</i>	<i>No</i>	<i>No</i>	<i>No</i>	<i>No</i> [‡]	Yes	Yes

Table 3: Bootstrap 95% confidence intervals (item-level paired resampling, 1,000 draws) for the headline columns of Table 1. Values are reported as point±half-width in percentage points. The bottom row indicates whether the best DrugClaw variant’s CI separates from the best baseline’s CI (no overlap = statistically significant lead at $\alpha=0.05$). [‡]On Faith. the DrugClaw-linear lower bound (.871) exceeds the next-best Direct LLM (GPT-5) upper bound (.843); however the ToolUniverse CI upper bound (.864) lies inside the DrugClaw-linear interval, so the lead over ToolUniverse is marginal. The *judge-mediated* EI columns and the judge-independent Primary column show no overlap with any baseline CI. The *closed-form* MedQA and PubMedQA leads, by contrast, fall inside the best-baseline CI band: we therefore characterise these tracks as *competitive* rather than statistically dominant, and note that the authority-aware Evidence Index is the load-bearing claim of Table 1.

Variant	(P, C, A)	best ^a	graph	Δ_{pp}
Default (paper)	(1.0, 0.7, 0.5)	0.513	0.632	+11.9
Uniform	(1.0, 1.0, 1.0)	0.555	0.642	+8.7
Harsher	(1.0, 0.3, 0.1)	0.477	0.620	+14.3
No upstream-of	(1.0, 0.7, 0.5)	0.512	0.620	+10.8

Table 4: Authority-weight and upstream-of sensitivity for the composite EI_{Llama}. P/C/A = bucket weight for primary / curated / aggregator. *Uniform* drops the primary-aggregator hierarchy; *Harsher* amplifies it; *No upstream-of* sets $\mathcal{U} = \emptyset$ so that an authoritative upstream citation no longer counts when the gold cites the downstream aggregator. *best*: best-baseline EI_{Llama}; *graph*: DrugClaw-graph EI_{Llama}. ^aBest baseline is Direct LLM (GPT-5) in every variant. DrugClaw-graph remains top-1 on EI_{Llama} across all four variants with leads in the +8.7 to +14.3 pp range.

D Robustness to Unparseable-Verdict Handling

The headline numbers in Table 1 follow standard LLM-as-judge practice and drop items where the judge emits an unparseable verdict from the judge-score numerator and denominator (§4.3). To verify that this choice does not produce spurious rankings, we re-compute the composite Evidence Index (Eq. 4) under an intention-to-treat (ITT) rule that instead counts every unparseable verdict as “No”. Under this rule the judge-score denominator returns to the full 3,772 items, matching the most adversarial common alternative used in the LLM-as-judge literature. Table 5 compares the two rules side by side.

System	EI _{Llama}		EI _{loss}	
	drop	ITT	drop	ITT
Direct LLM (GPT-5-mini)	0.430	0.430	0.403	0.400
Direct LLM (GPT-5)	0.513	<u>0.513</u>	0.494	<u>0.490</u>
ToolUniverse	0.357	0.357	0.340	0.339
Biomni	0.489	0.489	0.470	0.463
DeepEvidence	0.477	0.477	0.457	0.446
DrugClaw-linear	<u>0.626</u>	0.548	<u>0.591</u>	0.512
DrugClaw-graph	0.632	0.504	0.623	0.489

Table 5: Robustness of the composite Evidence Index to two unparseable-verdict handling rules. “drop” is the rule used in Table 1 (Unknown excluded from numerator and denominator). “ITT” is intention-to-treat (Unknown counted as “No”). Under both rules, DrugClaw takes top-1 on EI under both judges; only the best mode shifts from graph (under drop, where the higher unparseable rate of graph is hidden) to linear (under ITT, where it is penalised). Direct LLM (GPT-5) is the strongest baseline under both rules. **Bold** marks the column maximum; underline the runner-up.

The mode-level reordering is intuitive: graph mode produces multi-claim prose that the judges parse less reliably (47% to 50% unparseable versus 30% to 35% for linear, §5), so when unparseable verdicts are treated as “No” graph absorbs more cost than linear. At the system level, DrugClaw remains top-1 on EI under both judges and both rules, which is the property the metric is intended to support. The drop rule is reported in the main text because it is the protocol used by MT-Bench and follow-up LLM-as-judge work (Zheng et al.,

2023; Liu et al., 2023).

E Web-Search Fallback: Frequency and Impact

DrugClaw-graph retains a web-search fallback inside its reflector loop (Algorithm 1): when the reflector terminates with sufficiency $r_t < \tau_{\text{suff}}$ at the iteration bound T_{max} , the chain invokes a web-search step and re-runs the responder over the augmented evidence pool. The baselines (Biomni, DeepEvidence) are run under their released default configurations, which retrieve from each system’s bundled tool registry and knowledge bases and do not invoke open-web search for these queries (Appendix G); it is therefore important to quantify the impact of this asymmetry on DrugClaw’s reported numbers. The fallback fires on 894/3,772 (23.7%) of evidence dataset items, 80/751 (10.7%) of MedQA items, and 81/512 (15.8%) of PubMedQA items. DrugClaw-linear, by construction, never invokes the fallback (verified on all three datasets).

Citation-side impact. Table 6 compares the authority-aware metric panel on the fallback-fired subset of DrugAudit against the subset on which the reflector terminated naturally, and reports a counterfactual in which we disable the fallback (treat fallback items as if the system had refused, emitting no citation). The fallback fires precisely on items where the closed registry was insufficient; these items have substantially lower authority, faithfulness and primary-source rates than the no-fallback subset (0.20 vs. 0.49 for authority; 0.62 vs. 0.88 for faithfulness). Disabling the fallback entirely *improves* citation-side metrics slightly, because the fallback trades coverage for citation quality on the hardest items.

Closed-form impact. For the closed-form tracks, we estimate the no-fallback counterfactual by substituting DrugClaw-linear’s prediction (which never uses the fallback) on the items where graph mode fired the fallback. Under this substitution, DrugClaw-graph accuracy drops modestly from 0.920 to 0.917 on MedQA (−0.3 pp) and from 0.693 to 0.678 on PubMedQA (−1.6 pp); graph mode remains the top-1 system on both tracks under either configuration. The fallback is therefore not pivotal to the headline rankings; disabling it across the board would preserve every conclusion drawn in §5.

F Reproducibility

Hardware. Single GPU not required for inference. All seven systems were run on a CPU plus remote-API setup; the LLM calls were routed through an OpenAI-compatible inference gateway hosted on the authors’ institutional cluster (details anonymised for review).

Software. Python 3.11, OpenAI Python SDK 1.50+, pdftotext and beautifulsoup4 for skill data loaders. The state-machine orchestration is implemented on top of the LangGraph library; the contribution of DrugClaw is the agent composition, the typed evidence schema and the authority-aware metric panel rather than the orchestrator choice, so any equivalent state-machine library would suffice. The full skill registry and benchmark harness are released under an Apache-2.0 license at <https://anonymous.4open.science/r/DrugClaw-01A3/README.md>.

Cost. Total LLM spend across all candidate runs and all judge runs was approximately USD \$600 at GPT-5-mini and Llama / gpt-oss gateway rates.

G Baseline Configurations

Each compared system is run under its own released framework with no internal modifications; we control for two confounds at the interface layer: the planner backbone is fixed across systems for fairness, and the dataset-specific system prompt is shared verbatim across systems so that the candidate-side prompting surface contributes equally to every comparison. The per-system implementation choices are summarised in Table 7.

Inference endpoint. All systems and both judges route their calls through a single OpenAI-compatible inference gateway (institution anonymised for review; `api_mode = "responses"`). Per-call parameters are held constant across systems: `max_tokens = 40000`, `timeout = 100 s`, `temperature = 0.7` for candidate runs and `temperature = 0` for judge runs. Candidate runs use GPT-5-mini as the planner backbone (with GPT-5 for the upper-baseline Direct LLM); judge runs use llama-3.1-70b-instruct (primary) and gpt-oss-120b (secondary). Because the gateway and parameters are shared, the only sources of cross-system variance are the released framework code and the registry of tools each system invokes.

Metric	fb-fired ($n=894$)	no-fb ($n=2878$)	All ($n=3772$, current)	No-fb counterfactual
answered_rate	0.682	0.458	0.511	0.511
source_authority_rate	0.203	0.488	0.420	0.416
snippet_semantic_rate	0.172	0.382	0.332	0.335
source_primary_rate	0.802	0.931	0.918	0.931
faithfulness_rate	0.625	0.876	0.852	0.876
evidence_index_partial	0.411	0.641	0.596	0.601

Table 6: Web-search fallback impact on DrugClaw-graph citation-side metrics over DrugAudit. The “No-fb counterfactual” column reports the values that would be obtained if the web-fallback were disabled and the corresponding items returned no citation. Disabling the fallback *raises* primary, faithfulness and the citation-side evidence index by 1.2 to 2.4 pp, so the fallback is not an unfair lift but rather a small drag on the authority-aware panel.

System	Framework	Planner	Notes
Direct LLM (GPT-5-mini)	chat completion	GPT-5-mini	no tools; no retrieval.
Direct LLM (GPT-5)	chat completion	GPT-5	no tools; no retrieval.
ToolUniverse (Gao et al., 2024)	official 1.1.x	GPT-5-mini	108 tools loaded statically; native function-calling.
Biomni (Huang et al., 2025)	Stanford Biomni	GPT-5-mini	default biomedical-tool registry; data cached locally.
DeepEvidence (Wang et al., 2025)	BioDSA	GPT-5-mini	KBs: pubmed_papers, clinical_trials, drug, disease.
DrugClaw-linear	this work	GPT-5-mini	latency-prioritised subset of 19 skills from the 57-skill registry; no web search.
DrugClaw-graph	this work	GPT-5-mini	closed registry + reflector loop ($\tau_{\text{suff}}=0.7$, $T_{\text{max}}=2$); web fallback only on terminal insufficiency.

Table 7: Per-system implementation choices. The planner backbone is held fixed at GPT-5-mini for every agent and tool-augmented baseline; the upper-baseline Direct LLM (GPT-5) is included to bound the parametric-knowledge ceiling. Every system receives the same dataset-specific user prompt (§4) and writes its output into the same canonical JSON schema; agent frameworks whose internal templates fight the JSON requirement are post-processed by a normaliser LLM that re-emits the canonical schema without altering the answer content.

Default-configuration runs. Biomni and DeepEvidence are invoked under their released default configurations without modification to their tool registry: we neither enable nor disable any individual adapter, and at default each system retrieves from its bundled biomedical tools and knowledge bases rather than from open-web search. DrugClaw-graph retains a web-search fallback inside its reflector loop; we report in Appendix E the fraction of items for which the fallback fires and the counterfactual impact on the authority-aware panel of disabling it entirely. Two-stage agent systems whose internal prompt template enforces an alternative output schema (DrugClaw-graph, Biomni, DeepEvidence) emit their native answer plus already-extracted citations to a small normaliser LLM (GPT-5-mini) which re-emits the canonical JSON schema without altering answer content; the normalisation step is the same for every such system and never re-runs retrieval.

H Code Agent: Safe Sublanguage and Sandbox

This appendix expands the Code Agent specification summarised in §3.3. The agent emits a candidate program c in the safe Python sublanguage $\mathcal{L}_{\text{safe}}$, defined by three independent restrictions.

Banned AST nodes. Let \mathcal{B}_{ast} denote the set of AST node classes that disqualify a program from $\mathcal{L}_{\text{safe}}$:

$$\mathcal{B}_{\text{ast}} = \{ \text{While, With, AsyncWith, AsyncFor, AsyncFunctionDef, ClassDef, Global, Nonlocal, Lambda} \}.$$

A program containing any node in this set is rejected outright. The choice excludes unbounded iteration, side channels through global or non-local bindings, and dynamic function-definition tricks that would complicate static analysis.

Allowed imports. The agent may import only the four standard-library modules in $\mathcal{I}_{\text{ok}} =$

{json, math, re, statistics}. The first three cover JSON serialisation, numeric work and pattern matching, which together are sufficient for the great majority of skill-call patterns. The statistics module is useful for aggregating activity records (e.g. median IC_{50} across replicate assays). All other imports trigger rejection.

Allowed built-ins. The agent’s program runs in a globals dictionary whose built-ins are restricted to the curated allow-list \mathcal{F}_{ok} . The allow-list contains the exceptions `ValueError`, `TypeError`, `KeyError` and `IndexError`; the iteration helpers `len`, `range`, `min`, `max`, `sum`, `sorted`, `enumerate` and `zip`; the constructors `list`, `dict`, `set`, `tuple`, `str`, `int`, `float` and `bool`; the predicates `abs`, `all` and `any`; and `print`. The built-ins `exec`, `eval`, `open`, `compile`, `__import__`, `input`, `help`, `dir`, `globals`, `locals` and `vars` are all blocked at evaluation time.

Proxy-only sandbox. Even within \mathcal{L}_{safe} , an attacker could in principle attempt to traverse Python’s object model from the skill instance back into the host process (e.g. via `instance.__class__.__mro__`). The sandbox $\Sigma(K)$ therefore exposes the skill K through a proxy that intercepts attribute access on dunder-prefixed names and rejects access to `__class__`, `__globals__`, `__subclasses__` and the wider object-introspection ladder. A hard SIGALRM timeout, set per call by the DrugClaw runtime, aborts any execution that does not return within the configured budget.

Fallback semantics. If $c \notin \mathcal{L}_{safe}$, if proxy interception raises, or if the sandbox times out, the Code Agent invokes $K.retrieve(u)$ directly with the original subquery. The fallback ensures that retrieval is never silently lost, at the modest cost that the failure mode is logged but not surfaced to the user. In practice the validation pass rejects fewer than 1% of generated programs in our reported runs, and the timeout fires on fewer than 0.5% of skill calls.

I Operational Modes: Full Specification

DrugClaw ships in three reasoning modes that share the skill registry and entity-resolution layer of §3, the Code Agent of §3.3 and the output schema of §3.4, but differ in which operators of Eq. 1 are applied and in whether the retrieve-and-reason chain iterates. The summary in §3.2 gives the headline

definitions; this appendix reproduces the full pseudocode for each mode and a side-by-side comparison of the operator stacks they invoke.

Linear mode

Linear mode is the default deployment target for end-user-facing prose. It executes a single forward pass through the planner, Code Agent, and responder, omitting the graph builder, reranker, reflector and web-search fallback, and is summarised in Algorithm 2.

Algorithm 2 DrugClaw linear-mode workflow.

Require: query q ; skill registry \mathcal{R}
Ensure: answer a^* , evidence list \mathcal{E}^*
1: $\mathcal{P} \leftarrow \text{Plan}(q; \mathcal{R}_{\text{enabled}})$
2: $\mathcal{E} \leftarrow \bigcup_{u \in \mathcal{P}} \text{exec_sandbox}(\text{CodeAgent}(u))$
3: $a \leftarrow \text{Resp}(\mathcal{E}, q)$
4: **return** (a, \mathcal{E})

Equivalent to fixing $T_{\max} = 1$ in Eq. 1 and deleting the `GBld`, `Rerk` and `Refl` operators. Linear mode terminates after one round of skill execution even when the underlying retrieval returns no records; in that case the responder emits “I do not know” and the answer carries an empty `evidence_items` list. There is no web-search fallback. The mode prioritises latency over depth: median wall-clock time per item is 14 seconds (Appendix K), and the evidence pool seen by the responder is a flat union of retrieval results rather than a reranked subgraph.

Graph mode

Graph mode is the deeper retrieval-and-reason variant intended for analyst-facing multi-source exploration. It instantiates Eq. 1 in full: every operator (`Plan` \rightarrow `Retr` \rightarrow `GBld` \rightarrow `Rerk` \rightarrow `Resp` \rightarrow `Refl`) is applied at each iteration and the reflector controls termination. Algorithm 1 in §3.2 gives the full pseudocode; we reproduce the key control flow here for the appendix to be self-contained. The graph builder (`GBld`) materialises the retrieved records into a typed claim-evidence subgraph, the reranker (`Rerk`) reorders nodes by source-authority and relevance to the query plan, and the reflector (`Refl`) computes a sufficiency score $r_{t+1} = \rho_{t+1} - \lambda \max(0, r_t - \rho_{t+1})$ (Eq. 2). The loop iterates while $r_t < \tau_{\text{suff}} = 0.7$ and $t < T_{\max} = 2$; on terminal insufficiency the chain invokes the web-search fallback, re-runs the responder over the augmented evidence pool, and returns. The median wall-clock time per item is 46 seconds and the responder sees a graph with mean fan-out of 5.1

evidence records per answered claim (Appendix K, Appendix L).

Web-only mode

Web-only mode is intended for queries that fall outside the curated registry (e.g. recently approved drugs whose records have not propagated into the local skills). As specified in Algorithm 3, it bypasses the entire plan-retrieve-respond chain and routes q directly to the web-search agent.

Algorithm 3 DrugClaw web-only mode workflow.

Require: query q
Ensure: answer a^* , evidence list \mathcal{E}^*
 1: $\mathcal{E} \leftarrow \text{WebSearch}(q)$
 2: $a \leftarrow \text{Resp}(\mathcal{E}, q)$
 3: **return** (a, \mathcal{E})

Web-only mode is excluded from the comparison in §5 because DrugAudit is built against the closed registry of §3; including a web-search variant against this benchmark would conflate retrieval venue with retrieval depth.

Operator stacks at a glance

Table 8 contrasts which operators of Eq. 1 each mode invokes.

Operator	Linear	Graph	Web-only
Plan	✓	✓	×
Retr (skills)	✓	✓	×
WebSearch	×	on fallback only	✓
GBld	×	✓	×
Rerk	×	✓	×
Resp	✓	✓	✓
Refl (loop)	×	✓	×
Iter. bound T_{\max}	1	2	1
Suff. thresh. τ_{suff}	×	0.7	×

Table 8: Operators of Eq. 1 invoked by each reasoning mode. Linear collapses the loop to a single plan-retrieve-respond pass; graph runs the full operator stack with reflector-controlled iteration; web-only bypasses the skill registry and goes straight to web search.

Which mode to use

The headline numbers in Table 1 make graph mode the quality-maximising default and linear mode the operationally cheaper runner-up. Two practical considerations narrow this choice further. The LLM-judge parse rate on graph-mode outputs is substantially lower than on linear-mode outputs (47% to 50% unparseable verdicts versus 30% to 35%; §5), and any downstream LLM that consumes DrugClaw’s output (whether a summariser,

System	refusal rate	refusal \rightarrow Yes
Direct LLM (GPT-5-mini)	74.3%	5.1%
Direct LLM (GPT-5)	54.5%	4.9%
ToolUniverse	87.9%	4.3%
Biomni	49.0%	1.5%
DeepEvidence	37.3%	1.3%
DrugClaw-linear	41.1%	<u>91.1%</u>
DrugClaw-graph	48.3%	96.6%

Table 9: Refusal rate (fraction of items returned as “I do not know” or equivalent) and the fraction of those refusals, conditional on the LLM judge producing a parseable verdict, that score “Yes” because the gold itself reports no data. DrugClaw attains the highest calibration ratio among the seven systems by a wide margin, which reflects the reflector’s explicit “insufficient evidence” return-path triggering only when the underlying retrieval also fails.

a chatbot or an audit aggregator) will face the same parsing friction, so deployments that chain another model after the agent should prefer linear mode unless the consumer is explicitly tuned to multi-claim agent prose. Graph mode’s reflector also refuses more often (48.3% vs. 41.1% for linear; Appendix J) because the sufficiency threshold $\tau_{\text{suff}} = 0.7$ trades coverage for precision. Settings that need broader coverage at the cost of more partial answers can either run linear mode or lower τ_{suff} in graph mode; we do not tune τ_{suff} in this paper and leave its calibration frontier to future work.

J Calibrated Refusal: Extended Analysis

This appendix expands the refusal-behaviour analysis summarised in §6. Refusal rates and the fraction of refusals that receive judge verdict “Yes” (i.e. that align with a “no data” or “not reported” gold) are reported in Table 9.

Calibrated abstention is the operating point recommended by recent work on confidence in language models (Kadavath et al., 2022; Slobodkin et al., 2023; Varshney et al., 2023) when the alternative is plausible-sounding numeric confabulation. The amiodarone-EGFR case study reproduced in Appendix M illustrates the trade-off on a single item: when ChEMBL contains no bioactivity record for the drug-target pair, DrugClaw returns “I do not know” and the judge scores the response “Yes”; the strongest tool-augmented baseline fabricates a plausible μM -range IC_{50} instead and the judge scores it “No”.

K Cost and Latency

This appendix reports the per-item runtime and cost figures referenced in §6. DrugClaw-linear completes a query in 14 seconds (median, 2.4 skill calls) and DrugClaw-graph in 46 seconds (5.1 calls). Biomni takes 32 seconds with 4.7 calls and DeepEvidence 54 seconds with 6.2 calls; the direct language model returns in 3 to 7 seconds with no tools. The closed-registry design caches retrieval on disk, yielding per-item GPT-5-mini costs near \$0.012 for linear mode and \$0.025 for graph mode. The total spend across all candidate runs and both judge runs was approximately USD \$600 at GPT-5-mini, Llama-3.1-70B-Instruct and gpt-oss-120b gateway rates.

L Performance by Question Type

DrugAudit tags each item with a question-type label in the `meta.question_type` field. The labels group items by the cognitive operation the question requires rather than by the source database. Table 10 reports the per-(system, question-type) composite judge score $(\text{Yes} + 0.5 \cdot \text{Partial}) / (\text{Yes} + \text{Partial} + \text{No})$ under the Llama-3.1-70B-Instruct judge, consistent with the parseable-only denominator of §4.3. The Δ_{DC} column reports the gap between the best DrugClaw mode and the best baseline (positive = DrugClaw lead).

Evidence density and answer thoroughness.

On items that receive a substantive answer (i.e. not refused), DrugClaw-linear emits a mean of 3.78 citations per item and DrugClaw-graph emits a mean of 5.09. By comparison the tool-augmented baselines emit 1.43 (ToolUniverse) to 2.07 (Biomni) and the direct language model emits 1.72. The same ranking holds for median answer length: 327 characters for DrugClaw-linear against 135 to 206 for every baseline. These numbers indicate that for the subset of items DrugClaw chooses to answer, the response carries substantially more attached evidence and prose detail than any compared system, which is the deployment-side property that we expect a closed, provenance-strict registry to deliver.

M Case Studies

Each box reproduces system outputs verbatim. Citations (`source_db` + snippet head) are reproduced as recorded in the `evidence_items` field of DrugClaw’s output and in the corresponding citation

field of each baseline.

Case 1: FAERS exact-count retrieval. *ID:* faers-atenolol-attr-01. The question asks how many FAERS reports of NAUSEA are recorded for atenolol. The gold answer is 7,618.

Gold	“FAERS reports 7,618 reports of NAUSEA for atenolol.”
DrugClaw-linear	“... atenolol has 7,619 spontaneous reports of NAUSEA.” (cite: FAERS)
Biomni	“... 0 reports of ‘nausea’ were found for atenolol.”
DeepEvidence	“... there are 5,016,555 reports of NAUSEA for atenolol...”
Direct LLM (GPT-5)	“I don’t know.”

DrugClaw is off by 1 (−0.01%) because of a within-day data-snapshot timing difference. The two tool-augmented baselines issue plausible-looking openFDA queries but miss the `substance_name` normalisation step that the FAERS API requires; Biomni reads zero matches and DeepEvidence reads back the global NAUSEA row (every drug, ~5M reports).

Case 2: Orange Book brand-name lookup.

ID: orange_book-prednisone-verify-02. The question asks whether the FDA Orange Book lists PREDNISONE INTENSOL as an approved brand of prednisone. Gold: “Yes.”

Gold	“Yes, the FDA Orange Book lists PREDNISONE INTENSOL as a trade name for prednisone.”
DrugClaw-graph	“Yes. The FDA Orange Book lists PREDNISONE INTENSOL (ANDA088810), sponsor HIKMA, as an approved prednisone product.” (cite: FDA Orange Book)
Biomni	“No... returns no matching records, although the FDA Daily-Med label for prednisone...”
DeepEvidence	“No. The FDA... does not list ‘PREDNISONE INTENSOL’ as an approved brand...”
Direct LLM (GPT-5)	“No...”

The brand is listed in the Orange Book, but the baselines either ran an exact-string product lookup that missed the listing or fell back on parametric memory. DrugClaw accompanies its “Yes” with the ANDA number and the sponsor, both directly retrievable from the Orange Book skill, and the answer is auditable end-to-end.

Case 3: FAERS rare-event lookup. *ID:* faers-aripiprazole-attr-01. *Q:* “According to FAERS, how many reports of SUICIDE ATTEMPT are there for aripiprazole?” *Gold:* “1,517.”

Question type	What it measures	n	Baselines				DrugClaw		Δ_{DC}
			GPT-5	TU	Biomni	DeepEv.	linear	graph	
direct_lookup	single-fact retrieval	866	0.239	0.059	0.283	0.350	0.444	0.506	+0.156
attribute_specific	numeric attribute value	688	0.343	0.065	0.169	0.275	<u>0.651</u>	0.666	+0.323
yes_no_verify	yes/no with citation	918	0.505	0.131	0.343	<u>0.477</u>	0.394	0.318	-0.111
no_evidence	calibrated “no data”	917	0.479	0.284	0.529	0.674	0.972	<u>0.960</u>	+0.298
complementary_safety	safety overlap across sources	127	0.000	0.000	<u>0.394</u>	0.343	0.424	0.176	+0.030
convergent_indication	indication aggregation	115	0.922	0.452	0.543	0.630	<u>0.676</u>	0.130	-0.245
convergent_moa	mechanism convergence	65	0.700	0.231	0.608	0.592	<u>0.879</u>	0.885	+0.185
chained_target_disease	drug \rightarrow target \rightarrow disease	50	0.240	0.120	<u>0.420</u>	0.670	0.057	0.061	-0.609
convergent_adr	ADR aggregation across sources	26	0.077	0.000	<u>0.250</u>	0.038	0.286	<u>0.250</u>	+0.036

Table 10: Composite judge score per question type under the Llama judge. DrugClaw takes the top score on six of nine question types, with positive Δ_{DC} gaps ranging from +3 pp (*complementary_safety*, *convergent_adr*) to +32 pp (*attribute_specific*). The two modes are complementary: graph mode leads on the three types whose gold answers reward cross-record synthesis (*direct_lookup*, *attribute_specific*, *convergent_moa*); linear mode leads on the three types where the gold is a single fact or a calibrated “no data” refusal (*no_evidence*, *complementary_safety*, *convergent_adr*). Baselines lead on three types where the closed registry is at a structural disadvantage: GPT-5 on *yes_no_verify* and *convergent_indication*, both probing broad clinical-association recall where parametric memory is hard to beat without an open-web step; DeepEvidence on *chained_target_disease*, where its literature reach exceeds DrugClaw’s skill registry. Extending the registry with literature-mining tools is one direction Limitations identifies as future work. *GPT-5* = Direct LLM with GPT-5; *TU* = ToolUniverse.

DrugClaw-linear	“According to FAERS, there are 1,517 spontaneous reports...” (cite: FAERS)
Biomni	“I don’t know.”
DeepEvidence	“3,505 FAERS reports of ‘SUICIDE ATTEMPT’ for aripiprazole.”
Direct LLM (GPT-5)	“I don’t know.”

DeepEvidence’s 3,505 likely conflates reports with all related-event variants. The exact-match DrugClaw response is the deployable answer for a pharmacovigilance triage workflow.

“According to ChEMBL, what bioactivity is reported for amiodarone against EGFR?” *Gold*: “ChEMBL does not report any bioactivity of amiodarone against EGFR.”

DrugClaw-linear	“I don’t know.”
Biomni	“ChEMBL reports an IC50 of 10.0 μ M (10000 nM) for amiodarone inhibiting EGF-stimulated tyrosine phosphorylation of EGFR in A431 cells (activity_id 60162).”

Case 4: PharmGKB \rightarrow CPIC upstream citation.

ID: pharmgkb-atorvastatin-attr-01. *Q*: “According to PharmGKB, what is the level of evidence for the atorvastatin-SLCO1B1 (rs4149056) clinical annotation?” *Gold*: “Level of evidence 1A.”

DrugClaw-linear	“PharmGKB assigns level 1A evidence to the atorvastatin-SLCO1B1 (rs4149056) clinical annotation.” (cite: PharmGKB and CPIC)
-----------------	---

DrugClaw cites both PharmGKB and CPIC; the latter is the clinical-implementation arm of PharmGKB and a first-class primary record for prescribing guidelines. Under the legacy source-match rate the CPIC citation contributes zero because the gold string is the literal “PharmGKB”; under our authority-aware rule it counts as a primary upstream citation.

Case 5: Calibrated refusal on “no data” golds.

ID: chembl-amiodarone-no_evidence-03. *Q*:

ChEMBL does not contain the cited record (the activity ID does not resolve). Biomni’s confabulation is plausible at the surface, correct unit, correct cell line for EGFR assays, and a plausible IC₅₀ range, but is a hallucination. Under our judge prompt the calibrated refusal is scored “Yes” because the gold itself reports no data; the confabulation is scored “No”. In pharmacovigilance settings this asymmetry is appropriate, because a fluent fabrication of a kinase-activity number is a higher-risk failure mode than an honest refusal.

Case 6: openFDA Label warning extraction.

ID: openfda_label-clozapine-verify-02, *abridged*. *Q*: “Does the clozapine label include a boxed warning for agranulocytosis?” *Gold*: “Yes; boxed warning for severe neutropenia including agranulocytosis.”

DrugClaw-linear	“Yes; the openFDA Label for clozapine contains a boxed warning for severe neutropenia including agranulocytosis.” (cite: openFDA Label, boxed warning)
Direct LLM (GPT-5-mini)	“Yes; clozapine’s prescribing information warns about agranulocytosis.” (no citation)

The factual content matches but only DrugClaw points back at the specific Label section. In a clinical-decision-support setting, this is the difference between a recommendation a prescriber can verify against the FDA document in one click and one whose primary source they must look up by hand.

Case 7: Multi-source overlap query (multi-source aggregation; ID withheld for brevity).

Multi-source items in the benchmark explicitly mix records from ≥ 2 databases. DrugClaw-graph excels here because the agent’s claim-evidence graph (§3.2) walks across skills before synthesising: in our error analysis, 66.6% of multi-source items receive a substantive answer from DrugClaw-graph compared with 55 to 62% for the next-best tool-augmented systems. The single-claim Direct-LLM baselines lose the most here because each subclaim that requires a tool call is a separate failure point.